



Research article

Dynamics and density function of a HTLV-1 model with latent infection and Ornstein-Uhlenbeck process

Yan Ren, Yan Cheng*, Yuzhen Chai and Ping Guo

College of Mathematics, Taiyuan University of Technology, Taiyuan 030024, China

* **Correspondence:** Email: chengy79@163.com.

Abstract: This paper examines the propagation dynamics of a T-lymphoblastic leukemia virus type I (HTLV-1) infection model in a stochastic environment combined with an Ornstein-Uhlenbeck process. In conjunction with the theory of Lyapunov functions, we initially demonstrate the existence of a unique global solution to the model when initial values are positive. Subsequently, we establish a sufficient condition for the existence of a stochastic model stationary distribution. Based on this condition, the local probability density function expression of the model near the quasi-equilibrium point is solved by combining it with the Fokker-Planck equation. Subsequently, we delineate the pivotal conditions that precipitate the extinction of the disease. Finally, we select suitable data for numerical simulation intending to corroborate the theorem previously established.

Keywords: stochastic HTLV-1 infection model; Lyapunov function; ergodic stationary distribution; probability density function; extinction

Mathematics Subject Classification: 60H10, 37A50

1. Introduction

The human T-lymphoblastic leukemia virus (HTLV), the first human retrovirus to have been discovered in the late 1970s, belongs to the subfamily of retroviral RNA oncoviruses. These viruses can lead to chronic, lifelong infections, with the main subtypes being type I and type II. Despite being one of the few examples of human oncogenic viruses, it has received relatively little public attention [1, 2]. This may be attributable to its relatively low prevalence in high-income countries and the current high level of societal concern about the HIV epidemic. The most recent estimates of the total number of individuals infected with HTLV-1 are at least 30 million. Infection with HTLV-1 can result in serious and potentially fatal complications. The virus has been associated with a wide variety of clinical conditions, most notably adult T-cell leukemia/lymphoma (ATL) and a chronic and progressive neurological condition known as HTLV-1-associated myelopathy (HAM) [3, 4]. It

is estimated that less than 5% of individuals infected with HTLV-1 will develop these diseases. At the same time, the remainder are classified as "healthy carriers" who may also develop symptoms such as lung and bladder infections. Furthermore, an analysis revealed that HTLV-1 infection was associated with a 57% increase in all-cause mortality, including several inflammatory conditions such as uveitis, infectious dermatitis, and polyarthritis. There is currently no treatment for HTLV-1, and there is a lack of global screening for this infection. Risk assessment is further complicated by the development of adult T-cell lymphoma or HTLV-associated myelopathy [5–7].

The viral protein Tax is a key antigen expressed by cells effectively infected by HTLV-1. It is involved in the activation of the transcription of HTLV-1 genes and the proliferation of infected T cells [8]. Mathematical models can provide insight into the study of the disease, extending earlier relevant models in conjunction with the role of the viral protein Tax in the process of infection. This allows for the accounting of the highly dynamic interplay between viral expression and transcriptional latency. Li M Y and Lim A G [8] have differentiated the class of infected cells into two pools, latent and active, giving the following model based on HTLV-1 infection:

$$\begin{cases} \frac{dx(t)}{dt} = \lambda - dx(t) - \beta x(t)y(t), \\ \frac{du(t)}{dt} = \delta\beta x(t)y(t) + \eta ry(1 - \frac{x+u}{K}) - (\mu + \sigma)u(t), \\ \frac{dy(t)}{dt} = \sigma u(t) - ay(t), \end{cases} \quad (1.1)$$

combining $x(t) + u(t) \ll K$ and $dy(t) = [\sigma u(t) - ay(t)]dt$ calculates that $y(t) < \frac{\sigma K}{a}$. All parameters are assumed to be positive constants, and their biological significances are given in Table 1. A transfer diagram for the described interactions is shown in Figure 1.

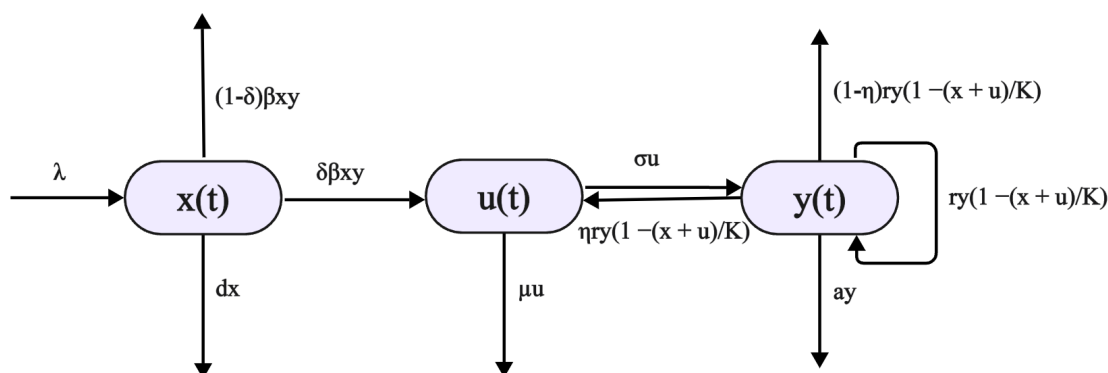


Figure 1. Transfer diagram describing the infection dynamics of HTLV-1 in vivo.

Table 1. Parameter meaning table.

parameter value	biological significance
$x(t)$	Number of healthy CD4 ⁺ helper T-cells at moment t,
$u(t)$	Number of CD4 ⁺ helper T-cells with latent infection (Tax-) at moment t,
$y(t)$	Number of CD4 ⁺ helper T-cells with active infection (Tax+) at moment t,
λ	CD4 ⁺ helper T-cell production rate,
β	Infectious transmission coefficient,
δ	Proportion of infected target cells surviving infectious transmission,
η	Proportion of infected target cells surviving mitotic propagation,
r	Tax-driven selective proliferation rate of actively infected target cells,
σ	Spontaneous Tax-expression rate,
d	Natural mortality of healthy target cells,
μ	Natural mortality of latently infected target cells,
a	Natural mortality of actively infected targets,
K	CD4 ⁺ helper T-cell carrying capacity.

Mathematical models provide valuable insights into the complex dynamics of disease transmission, forming a critical foundation for public health policy. Many scholars have developed theoretical studies on various deterministic infectious disease models [9–11]. Research on HTLV-1 dynamics has also yielded significant results. Wang and Ma [12] investigated the global kinetics of the HTLV-1 infection response-diffusion model considering factors such as mitotic division of infected cells and CTL immune response; Khajanchi et al. [13] investigated a mathematical model of CD8⁺ T cell response to HTLV-1 and performed a sensitivity analysis to explore the dynamic response to HTLV-1 infection and its role in the pathogenesis of HTLV-1-associated myelopathy/tropical spastic paralysis (HAM/TSP); Wang et al. [14] developed a model incorporating two time delays, showing through numerical simulations that intracellular delays stabilize the infection's steady state, while immune response delays can destabilize it. They also noted that intracellular delay affects both the magnitude and the time required for convergence to the steady state. These studies have significantly advanced the understanding of HTLV-1 dynamics.

As the complexity of epidemiological modeling increases, researchers are increasingly inclined to introduce stochastic factors to improve the predictive power and accuracy of models. In recent years, Bayesian filtering (especially Kalman filtering and particle filtering) has become an important tool for quantifying and estimating stochasticity in dynamical systems, and has been widely used especially in epidemiological modelling. Vasileios E Papageorgiou et al. [15] proposed a novel particle filtering method for assessing the dynamics of monkeypox outbreaks; Calvetti D et al. [16] focused on Bayesian particle filtering-based dynamic epidemic transmission models, especially for COVID-19, and the study showed that the algorithm has significant accuracy in estimating the proportion of latently infected individuals through computer simulations and experiments with real data; Jos Elfring et al. [17] discussed the popularization and application of the standard algorithm for particle filtering. On the other hand, Markov methods also have important applications in describing stochasticity in the spread of infectious diseases, and Artalejo JR et al. [18] provide insights into the computational methods of stochastic SEIR models and provide powerful tools for analyzing stochastic behavior during disease transmission. These methods can not only enhance the predictive performance

of existing epidemiological models, but can also be applied to other public health problems with uncertainty and dynamic evolution.

In real life, various organisms and populations are inevitably affected by the external environment. The presence of environmental noise means that parameters such as birth and death rates are subject to some kind of random perturbation. Several different types of stochastic epidemiological kinetic models have been developed and extensively studied. There are broadly two approaches in the existing literature to describe random effects in reality: Either linear perturbations or Ornstein-Uhlenbeck processes [19–21]. The Ornstein-Uhlenbeck process is a mathematical model that describes the evolution of random variables with mean-reverting properties. It can be used to simulate dynamical systems that exhibit short-term fluctuations and long-run convergence to the mean. Edward Allen [22] reviews two commonly used methods for incorporating environmental change factors into models of biological systems and concludes that the mean reversion process has some advantages over linear functions of white noise in modifying environmental change parameters. Zhou Baoquan et al. [23] formulated and studied a stochastic epidemic model with media coverage and two mean-reverting Ornstein-Uhlenbeck processes, and investigated the effects of random noise and media coverage on the spread of epidemics. Cai Yongli et al. [24] showed through their study that the Ornstein-Uhlenbeck process is a well-established method for introducing stochastic environmental noise into biologically realistic population dynamics models. Su Tan et al. [25] considered a stochastic SEIV epidemic model incorporating vaccination and general morbidity and derived a density function around the equilibrium point. Shi Z, Jiang D [26] studied a stochastic HIV model in which the parameters were perturbed by the Ornstein-Uhlenbeck process. The process is also described in the literature [27–29].

In this article the infection rate β in the system (1.1) is subject to fluctuations due to environmental noise, oscillating around the mean value $\bar{\beta}$. To model natural fluctuations in the infection rate β over time or changes in environmental factors, we treat it as a random variable. Define $\beta(t)$ as a stochastic process that varies over time [30]:

$$d\beta = \alpha(\bar{\beta} - \beta)dt + \theta dB(t),$$

where $\bar{\beta}$ is a positive constant representing $\beta(t)$ averaged over the long term, α denotes the rate of mean reversion, $B(t)$ stands for Standard Brownian Motion, and θ denotes the intensity of white noise. In this paper, $B(t)$ is defined on $\{\Omega, \{\mathcal{F}_t\}_{t \geq 0}, \mathbb{P}\}$, which is a complete probability space with filtration $\{\mathcal{F}_t\}_{t \geq 0}$ satisfying the incremental and right-continuous. \mathcal{F}_0 contains all \mathbb{P} -empty sets. Solving the above equation gives $\beta(t) = \bar{\beta} + (\beta(0) - \bar{\beta})e^{-\alpha t} + \theta \int_0^t e^{-\alpha(t-s)} dB(s)$, calculating the expectation and variance of $\beta(t)$ separately, we have

$$E(\beta(t)) = \bar{\beta} + (\beta(0) - \bar{\beta})e^{-\alpha t}, \text{Var}(\beta(t)) = \theta^2 \int_0^t e^{-2\alpha(t-s)} ds = \frac{\theta^2}{2\alpha}(1 - e^{-2\alpha t}),$$

when $t \rightarrow 0^+$, we have $E(\beta(t)) \rightarrow \beta(0)$ and $\text{Var}(\beta(t)) \rightarrow 0$, and it can be seen that it is reasonable to use the Ornstein-Uhlenbeck process to describe the evolution of the infection rate β over time under the influence of noise.

Thus, we can obtain a stochastic kinetic model for HTLV-1 infection:

$$\begin{cases} dx = [\lambda - dx - \beta^+ xy] dt, \\ du = \left[\beta^+ \delta xy + \eta ry \left(1 - \frac{x+u}{K}\right) - (\mu + \sigma)u \right] dt, \\ dy = (\sigma u - ay) dt, \\ d\beta = \alpha [\bar{\beta} - \beta(t)] dt + \theta dB(t), \end{cases} \quad (1.2)$$

where $\beta^+ = \max\{\beta(t), 0\}$, combined with the above analyses, the feasible domain of system (1.2) is

$$\Gamma := \{(x, u, y, \beta) \in \mathbb{R}_+^3 \times \mathbb{R} : x + u \leq K, y < \frac{\sigma K}{a}\}.$$

In this paper, we develop techniques and theory for threshold dynamics of stochastic model (1.2) incorporating the Ornstein-Uhlenbeck process, including the theory of uniqueness of the existence of global solutions in Section 2 and sufficient conditions for the existence of a stationary distribution of the system (1.2) in Section 3. Meanwhile, we further give the solution theory of special algebraic equations and the exact expression of the local probability density function of the system (1.2), and finally verify the correctness of our theory using numerical simulations.

2. Existence uniqueness of the global solution

Theorem 2.1 *For any initial values $(x(0), u(0), y(0), \beta(0)) \in \Gamma$, the system (1.2) has a unique global solution $(x(t), u(t), y(t), \beta(t))$, and is maintained with probability one in Γ .*

Proof. It is evident that the coefficients of the system (1.2) satisfy the local Lipschitz condition. Consequently, there exists a unique solution for $t \in [0, \tau_e)$, where τ_e represents the moment of explosion [30]. Let $R_n = (-n, -n) \times (-n, -n) \times (-n, -n) \times (-n, -n)$, for any initial value $(x(0), u(0), y(0), \beta(0)) \in \Gamma$, there exists a sufficiently large integer m_0 satisfying $(\ln x(0), \ln u(0), \ln y(0), \beta(0)) \in R_{m_0}$, for any $m \geq m_0$, define $\tau_m = \inf\{t \in (0, \tau_e) | (\ln x(t), \ln u(t), \ln y(t), \beta(t)) \notin R_m\}$, it is clear that τ_m is an increasing function concerning m . In the subsequent proof, we define $\inf\{\emptyset\} = +\infty$, $\tau_\infty = \lim_{m \rightarrow +\infty} \tau_m$; hence $\tau_\infty \leq \tau_e$. The following proves that $\tau_\infty = +\infty$ and thus can show that $\tau_e = +\infty$.

Adoption of the counterfactual: Assumptions $\tau_\infty \neq +\infty$, there exists $0 < \varepsilon_0 < 1$ and a positive constant m^* , $T_0 > 0$ satisfying

$$P(\tau_m \leq T_0) := P(G_m) \geq \varepsilon, \quad \forall m \geq m^*, \quad (2.1)$$

where $G_m = \{\tau_m \leq T_0 | (\ln x(t), \ln u(t), \ln y(t), \beta(t)) \notin R_m, t \in (0, \tau_m)\}$, defining non-negative functions

$$V = x - 1 - \ln x + u - 1 - \ln u + y - 1 - \ln y + \frac{\beta^2}{2},$$

combined with the Itô formula [30]:

$$\begin{aligned} LV &= \left(1 - \frac{1}{x}\right)(\lambda - dx - \beta^+ xy) + \left(1 - \frac{1}{u}\right)\left[\beta^+ \delta xy + \eta ry \left(1 - \frac{x+u}{K}\right)\right] - (\mu + \sigma)u + \left(1 - \frac{1}{y}\right)(\sigma u - ay) \\ &\quad + \alpha\beta(\bar{\beta} - \beta) + \frac{1}{2}\theta^2 \end{aligned}$$

$$\begin{aligned}
&= \lambda - dx - \beta^+ xy - \frac{\lambda}{x} + d + \beta^+ y + \delta\beta^+ xy + \eta ry - \frac{\eta ry(x+u)}{K} - (\mu + \sigma)u - \frac{\delta\beta^+ xy}{u} - \frac{\eta ry}{u} \left(1 - \frac{x+u}{K}\right) \\
&\quad + \mu + \sigma + \sigma u - ay - \frac{\sigma u}{y} + a + \alpha\beta(\bar{\beta} - \beta) + \frac{1}{2}\theta^2 \\
&\leq \lambda + d + \beta^+ y + \delta\beta^+ xy + \eta ry + \mu + \sigma + \sigma u + a + \alpha\beta(\bar{\beta} - \beta) + \frac{1}{2}\theta^2 \\
&\leq \beta^+ \left[\frac{\sigma K}{a}(1 + \delta K)\right] + \lambda + \frac{\eta\sigma r K}{a} + d + \mu + \sigma + \sigma K + \alpha\beta(\bar{\beta} - \beta) + \frac{1}{2}\theta^2 \\
&\leq [\alpha\bar{\beta} + \frac{\sigma K}{a}(1 + \delta K)]|\beta| - \alpha|\beta|^2 + \frac{\eta\sigma r K}{a} + \lambda + d + \mu + \sigma(1 + K) + \frac{1}{2}\theta^2 \\
&\leq A + \frac{\eta\sigma r K}{a} + \lambda + d + \mu + \sigma(1 + K) + \frac{1}{2}\theta^2 := D,
\end{aligned}$$

where

$$A = \sup_{\beta \in \mathbb{R}} \left\{ [\alpha\bar{\beta} + \frac{\sigma K}{a}(1 + \delta K)]|\beta| - \alpha|\beta|^2 \right\}.$$

Integrating and taking the expectation gives

$$\begin{aligned}
0 &\leq \mathbb{E}[V(x(\tau_m \wedge T_0), u(\tau_m \wedge T_0), y(\tau_m \wedge T_0), \beta(\tau_m \wedge T_0))] \\
&= \mathbb{E}[V(x(0), u(0), y(0), \bar{\beta})] + \mathbb{E}\left[\int_0^{\tau_m \wedge T_0} LV(x(\tau), u(\tau), y(\tau), \beta(\tau))d\tau\right] \\
&\leq \mathbb{E}[V(x(0), u(0), y(0), \bar{\beta})] + DT_0,
\end{aligned}$$

combined with Eq (2.1), for any $\xi \in G_m$, we get $V(x(\tau_m, \xi), u(\tau_m, \xi), y(\tau_m, \xi), \beta(\tau_m, \xi))$ outweigh $(e^m - 1 - m) \wedge (e^{-m} - 1 + m) \wedge \frac{m^2}{2}$, so

$$\begin{aligned}
\mathbb{E}[V(x(0), u(0), y(0), \beta(0))] + DT_0 &\geq \mathbb{E}[V(x(\tau_m \wedge T_0), u(\tau_m \wedge T_0), y(\tau_m \wedge T_0), \beta(\tau_m \wedge T_0))] \\
&\geq \mathbb{E}[1_{G_m(\xi)} V(x(\tau_m \wedge T_0), u(\tau_m \wedge T_0), y(\tau_m \wedge T_0), \beta(\tau_m \wedge T_0))] \\
&\geq P(G_m(\xi)) V(x(\tau_m, \xi), u(\tau_m, \xi), y(\tau_m, \xi), \beta(\tau_m, \xi)) \\
&\geq \varepsilon_0 [(e^m - 1 - m) \wedge (e^{-m} - 1 + m) \wedge \frac{m^2}{2}],
\end{aligned}$$

let $m \rightarrow \infty$, which gives

$$+\infty \leq \mathbb{E}V(x(0), u(0), y(0), \beta(0)) + DT_0 < +\infty,$$

this is a contradictory assertion, which invalidates our original assumption, i.e., $\tau_\infty = +\infty$. Therefore, there exists a unique global solution $(x(t), u(t), y(t), \beta(t))$ for the system (1.2).

3. Existence of a stationary distribution

In contrast to deterministic models, stochastic models lack positive equilibria. Consequently, this section will investigate whether the stochastic model (1.2) exhibits a stationary distribution indicative of the persistence of the epidemic.

Theorem 3.1. *If*

$$R_0^s = \frac{\delta\lambda\sigma\hat{\beta}}{a(\mu + \sigma)(d + \frac{\theta\sigma K}{2a\sqrt{\pi a}})} > 1,$$

then there exists a stationary distribution for system (1.2). Where

$$\hat{\beta} = \left(\int_{-\infty}^{\infty} (x \vee 0)^{\frac{1}{3}} \pi(x) dx \right)^3 = \left(\frac{1}{\sqrt{\pi}} \int_{-\frac{\bar{\beta}\sqrt{\alpha}}{\theta}}^{\infty} \left(\frac{\theta}{\sqrt{\alpha}} x + \bar{\beta} \right)^{\frac{1}{3}} e^{-x^2} dx \right)^3.$$

Proof. Taking the function $V_1 = -\ln u - c_1 \ln x - c_2 \ln y$, applying the Itô formula yields

$$\begin{aligned} LV_1 &= -\frac{\delta\beta^+ xy}{u} - \frac{\eta ry}{u} \left(1 - \frac{x+u}{K}\right) + \mu + \sigma - c_1 \frac{\lambda}{x} + c_1 d + c_1 \beta^+ y - c_2 \frac{\sigma u}{y} + c_2 a \\ &\leq -3 \sqrt[3]{\frac{\delta\beta^+ xy}{u} \times \frac{c_1 \lambda}{x} \times \frac{c_2 \sigma u}{y}} - \frac{\eta ry}{u} \left(1 - \frac{x+u}{K}\right) + \mu + \sigma + c_1 d + c_1 \beta^+ y + c_2 a \\ &= -3 \sqrt[3]{\delta c_1 c_2 \lambda \sigma \beta^+} + c_1 d + c_1 [P(t) + \bar{\beta}] y + c_2 a - \frac{\eta ry}{u} \left(1 - \frac{x+u}{K}\right) + \mu + \sigma \\ &\leq -3 \sqrt[3]{\delta c_1 c_2 \lambda \sigma \beta^+} + c_1 d + c_1 (P(t) \vee 0) \frac{\sigma K}{a} + c_2 a + c_1 \bar{\beta} y + \mu + \sigma \\ &\leq -3 \sqrt[3]{\delta c_1 c_2 \lambda \sigma \beta^+} + c_1 d + \frac{c_1 \theta \sigma K}{2a \sqrt{\pi \alpha}} + c_2 a + c_1 \bar{\beta} y + \mu + \sigma + \frac{c_1 \sigma K}{a} (P(t) \vee 0 - \int_0^{\infty} x \widehat{\pi}(x) dx) \\ &= -3 \sqrt[3]{\delta c_1 c_2 \lambda \sigma \hat{\beta}} + (3 \sqrt[3]{\delta c_1 c_2 \lambda \sigma \hat{\beta}} - 3 \sqrt[3]{\delta c_1 c_2 \lambda \sigma \beta^+}) + c_1 \left(d + \frac{\theta \sigma K}{2a \sqrt{\pi \alpha}}\right) + c_2 a + c_1 \bar{\beta} y + \mu + \sigma \\ &\quad + \frac{c_1 \sigma K}{a} (P(t) \vee 0 - \int_0^{\infty} x \widehat{\pi}(x) dx), \end{aligned}$$

where $P(t) = \beta(t) - \bar{\beta}$, seek to solve

$$\frac{\delta c_1 c_2 \lambda \sigma \hat{\beta}}{c_1 c_2 a \left(d + \frac{\theta \sigma K}{2a \sqrt{\pi \alpha}}\right)} = c_1 \left(d + \frac{\theta \sigma K}{2a \sqrt{\pi \alpha}}\right) = c_2 a,$$

we can have

$$c_1 = \frac{\lambda \delta \sigma \hat{\beta}}{a \left(d + \frac{\theta \sigma K}{2a \sqrt{\pi \alpha}}\right)^2}, \quad c_2 = \frac{\lambda \delta \sigma \hat{\beta}}{a^2 \left(d + \frac{\theta \sigma K}{2a \sqrt{\pi \alpha}}\right)},$$

consequently

$$\begin{aligned} LV_1 &\leq -\frac{\delta \lambda \sigma \hat{\beta}}{a \left(d + \frac{\theta \sigma K}{2a \sqrt{\pi \alpha}}\right)} + \mu + \sigma + c_1 \bar{\beta} y + 3 \sqrt[3]{\delta c_1 c_2 \lambda \sigma} (\sqrt[3]{\hat{\beta}} - \sqrt[3]{\beta^+}) + \frac{c_1 \sigma K}{a} (P(t) \vee 0 - \int_0^{\infty} x \widehat{\pi}(x) dx) \\ &= -(\mu + \sigma)(R_0^s - 1) + c_1 \bar{\beta} y + 3 \sqrt[3]{\delta c_1 c_2 \lambda \sigma} (\sqrt[3]{\hat{\beta}} - \sqrt[3]{\beta^+}) + \frac{c_1 \sigma K}{a} (P(t) \vee 0 - \int_0^{\infty} x \widehat{\pi}(x) dx), \end{aligned}$$

where

$$R_0^s = \frac{\delta \lambda \sigma \hat{\beta}}{a(\mu + \sigma) \left(d + \frac{\theta \sigma K}{2a \sqrt{\pi \alpha}}\right)}, \quad \hat{\beta} = \left(\int_{-\infty}^{\infty} (x \vee 0)^{\frac{1}{3}} \pi(x) dx \right)^3 = \left(\frac{1}{\sqrt{\pi}} \int_{-\frac{\bar{\beta}\sqrt{\alpha}}{\theta}}^{\infty} \left(\frac{\theta}{\sqrt{\alpha}} x + \bar{\beta} \right)^{\frac{1}{3}} e^{-x^2} dx \right)^3.$$

The function $V_2 = V_1 + \frac{c_1 \bar{\beta}}{a} y$ is taken, and the Itô formula is applied, which yields

$$LV_2 = LV_1 + \frac{c_1 \bar{\beta}}{a} u - c_1 \bar{\beta} y$$

$$\begin{aligned} &\leq -(\mu + \sigma)(R_0^s - 1) + c_1\bar{\beta}y + 3\sqrt[3]{\delta c_1 c_2 \lambda \sigma}(\sqrt[3]{\hat{\beta}} - \sqrt[3]{\beta^+}) + \frac{c_1\sigma K}{a}(P(t) \vee 0 - \int_0^\infty x\widehat{\pi}(x)dx) + \frac{c_1\sigma\bar{\beta}}{a}u - c_1\bar{\beta} \\ &= -(\mu + \sigma)(R_0^s - 1) + 3\sqrt[3]{\delta c_1 c_2 \lambda \sigma}(\sqrt[3]{\hat{\beta}} - \sqrt[3]{\beta^+}) + \frac{c_1\sigma K}{a}(P(t) \vee 0 - \int_0^\infty x\widehat{\pi}(x)dx) + \frac{c_1\sigma\bar{\beta}}{a}u. \end{aligned}$$

Taking the function $V_3 = -\ln x - \ln y - \ln(K - x - u) + \frac{\beta^2}{2}$, applying the Itô formula yields

$$\begin{aligned} LV_3 &= -\frac{\lambda}{x} + d + \beta^+y - \frac{\sigma u}{y} + a + \frac{\lambda}{K - x - u} - \frac{dx}{K - x - u} - \frac{\beta^+xy}{K - x - u} + \frac{\delta\beta^+xy}{K - x - u} + \frac{\eta ry}{K} \\ &\quad - \frac{(\mu + \sigma)u}{K - x - u} + \beta[\alpha(\bar{\beta} - \beta)] + \frac{\theta^2}{2} \\ &\leq -\frac{\lambda}{x} - \frac{\sigma u}{y} - \frac{dx}{K - x - u} + \frac{\sigma K}{a}|\beta| + \alpha\beta\bar{\beta} - \alpha\beta^2 + \frac{\theta^2}{2} + B, \end{aligned}$$

where

$$B = \sup_{(x,u,y,\beta) \in \mathbb{R}^3 \times \mathbb{R}^+} \left\{ \frac{\lambda}{K - x - u} + \frac{\delta\beta^+xy}{K - x - u} - \frac{\beta^+xy}{K - x - u} + \frac{\eta r\sigma}{a} + d + a \right\}.$$

Taking the function $\bar{V} = MV_2 + V_3$, the function has a minimum point in the feasible domain $\bar{V}(x_0, u_0, y_0, \beta_0)$, so we make $V = \bar{V} - \bar{V}(x_0, u_0, y_0, \beta_0)$, applying the Itô formula to it gives

$$\begin{aligned} LV &\leq -M(\mu + \sigma)(R_0^s - 1) + \frac{c_1\sigma\bar{\beta}M}{a}u + 3M\sqrt[3]{\delta c_1 c_2 \lambda \sigma}(\sqrt[3]{\hat{\beta}} - \sqrt[3]{\beta^+}) + \frac{c_1\sigma KM}{a}(P(t) \vee 0 - \int_0^\infty x\widehat{\pi}(x)dx) \\ &\quad - \frac{\lambda}{x} - \frac{\sigma u}{y} - \frac{dx}{K - x - u} + \frac{\sigma K}{a}|\beta| + \alpha\beta\bar{\beta} - \alpha\beta^2 + \frac{\theta^2}{2} + B \\ &:= F(x, u, y, \beta) + 3M\sqrt[3]{\delta c_1 c_2 \lambda \sigma}(\sqrt[3]{\hat{\beta}} - \sqrt[3]{\beta^+}) + \frac{c_1\sigma KM}{a}(P(t) \vee 0 - \int_0^\infty x\widehat{\pi}(x)dx), \end{aligned} \quad (3.1)$$

where

$$F(x, u, y, \beta) = -M(\mu + \sigma)(R_0^s - 1) + \frac{c_1\sigma\bar{\beta}M}{a}u - \frac{\lambda}{x} - \frac{\sigma u}{y} - \frac{dx}{K - x - u} + \frac{\sigma K}{a}|\beta| + \alpha\beta\bar{\beta} - \alpha\beta^2 + \frac{\theta^2}{2} + B.$$

Next, we first verify that related properties of $F(x, u, y, \beta)$, defining bounded closed sets

$$D_\varepsilon = \{(x, u, y, \beta)^T \in \Gamma : x \geq \varepsilon, u \geq \varepsilon, y \geq \varepsilon^2, x + u \leq K - \varepsilon^2, |\beta| \leq \frac{1}{\varepsilon}\} := \bar{D}_\varepsilon \times [-\frac{1}{\varepsilon}, \frac{1}{\varepsilon}],$$

divide the set $\Gamma \setminus D_\varepsilon$ into the following five regions:

$$\begin{aligned} D_{\varepsilon,1}^c &= \{(x, u, y, \beta)^T \in \Gamma : x < \varepsilon\}, \\ D_{\varepsilon,2}^c &= \{(x, u, y, \beta)^T \in \Gamma : u < \varepsilon\}, \\ D_{\varepsilon,3}^c &= \{(x, u, y, \beta)^T \in \Gamma : y < \varepsilon^2, u \geq \varepsilon\}, \\ D_{\varepsilon,4}^c &= \{(x, u, y, \beta)^T \in \Gamma : x + u > K - \varepsilon^2, x \geq \varepsilon\}, \\ D_{\varepsilon,5}^c &= \{(x, u, y, \beta)^T \in \Gamma : |\beta| > \frac{1}{\varepsilon}\}, \end{aligned}$$

meet the conditions:

$$-M(\mu + \sigma)(R_0^s - 1) + G_1 \leq -2, \quad (3.2)$$

$$-2 + \frac{c_1 \sigma \bar{\beta} M}{a} \varepsilon \leq -1, \quad (3.3)$$

$$-2 + \frac{c_1 \sigma \bar{\beta} M K}{a} - \frac{\lambda}{\varepsilon} \leq -1, \quad (3.4)$$

$$-2 + \frac{c_1 \sigma \bar{\beta} M K}{a} - \frac{\sigma}{\varepsilon} \leq -1, \quad (3.5)$$

$$-2 + \frac{c_1 \sigma \bar{\beta} M K}{a} - \frac{d}{\varepsilon} \leq -1, \quad (3.6)$$

$$-2 + \frac{c_1 \sigma \bar{\beta} M K}{a} - \frac{\alpha}{2\varepsilon^2} \leq -1, \quad (3.7)$$

where

$$G_1 = \sup_{\beta \in \mathbb{R}^+} \left\{ \frac{\sigma K}{a} |\beta| + \alpha \beta \bar{\beta} - \frac{\alpha}{2} \beta^2 \right\} + \frac{\theta^2}{2} + B < \infty.$$

Case 1. Consider the region $D_{\varepsilon,1}^c$,

$$\begin{aligned} F(x, u, y, \beta) &\leq -M(\mu + \sigma)(R_0^s - 1) + \frac{c_1 \sigma \bar{\beta} M}{a} u - \frac{\lambda}{x} + \frac{\sigma K}{a} |\beta| + \alpha \beta \bar{\beta} - \alpha \beta^2 + \frac{\theta^2}{2} + B \\ &\leq -\frac{\lambda}{x} - M(\mu + \sigma)(R_0^s - 1) + \frac{c_1 \sigma \bar{\beta} M K}{a} + \frac{\sigma K}{a} |\beta| + \alpha \beta \bar{\beta} - \alpha \beta^2 + \frac{\theta^2}{2} + B \\ &\leq -2 + \frac{c_1 \sigma \bar{\beta} M K}{a} - \frac{\lambda}{\varepsilon} \leq -1. \end{aligned}$$

Case 2. Consider the region $D_{\varepsilon,2}^c$,

$$\begin{aligned} F(x, u, y, \beta) &\leq -M(\mu + \sigma)(R_0^s - 1) + \frac{c_1 \sigma \bar{\beta} M}{a} u + \frac{\sigma K}{a} |\beta| + \alpha \beta \bar{\beta} - \alpha \beta^2 + \frac{\theta^2}{2} + B \\ &\leq -M(\mu + \sigma)(R_0^s - 1) + \frac{c_1 \sigma \bar{\beta} M}{a} \varepsilon + \frac{\sigma K}{a} |\beta| + \alpha \beta \bar{\beta} - \alpha \beta^2 + \frac{\theta^2}{2} + B \\ &\leq -2 + \frac{c_1 \sigma \bar{\beta} M}{a} \varepsilon \leq -1. \end{aligned}$$

Case 3. Consider the region $D_{\varepsilon,3}^c$,

$$\begin{aligned} F(x, u, y, \beta) &\leq -M(\mu + \sigma)(R_0^s - 1) + \frac{c_1 \sigma \bar{\beta} M}{a} u - \frac{\sigma u}{y} + \frac{\sigma K}{a} |\beta| + \alpha \beta \bar{\beta} - \alpha \beta^2 + \frac{\theta^2}{2} + B \\ &\leq -\frac{\sigma u}{y} - M(\mu + \sigma)(R_0^s - 1) + \frac{c_1 \sigma \bar{\beta} M K}{a} + \frac{\sigma K}{a} |\beta| + \alpha \beta \bar{\beta} - \alpha \beta^2 + \frac{\theta^2}{2} + B \\ &\leq -2 + \frac{c_1 \sigma \bar{\beta} M K}{a} - \frac{\sigma}{\varepsilon} \leq -1. \end{aligned}$$

Case 4. Consider the region $D_{\varepsilon,4}^c$,

$$F(x, u, y, \beta) \leq -M(\mu + \sigma)(R_0^s - 1) + \frac{c_1 \sigma \bar{\beta} M}{a} u - \frac{dx}{K - x - u} + \frac{\sigma K}{a} |\beta| + \alpha \beta \bar{\beta} - \alpha \beta^2 + \frac{\theta^2}{2} + B$$

$$\begin{aligned} &\leq -\frac{dx}{K-x-u} - M(\mu + \sigma)(R_0^s - 1) + \frac{c_1\sigma\bar{\beta}MK}{a} + \frac{\sigma K}{a}|\beta| + \alpha\beta\bar{\beta} - \alpha\beta^2 + \frac{\theta^2}{2} + B \\ &\leq -2 + \frac{c_1\sigma\bar{\beta}MK}{a} - \frac{d}{\varepsilon} \leq -1. \end{aligned}$$

Case 5. Consider the region $D_{\varepsilon,5}^c$,

$$\begin{aligned} F(x, u, y, \beta) &\leq -M(\mu + \sigma)(R_0^s - 1) + \frac{c_1\sigma\bar{\beta}M}{a}u - \frac{\alpha}{2}\beta^2 + \frac{\sigma K}{a}|\beta| + \alpha\beta\bar{\beta} - \frac{\alpha}{2}\beta^2 + \frac{\theta^2}{2} + B \\ &\leq -2 + \frac{c_1\sigma\bar{\beta}MK}{a} - \frac{\alpha}{2\varepsilon^2} \leq -1. \end{aligned}$$

Thus, there exists a sufficiently small ε satisfying that for any $(x, u, y, \beta) \in \Gamma \setminus D_\varepsilon$ there is $F(x, u, y, \beta) \leq -1$, and it can be demonstrated that there exists a positive constant number H satisfying the following condition: for any $(x, u, y, \beta) \in D_\varepsilon$ has

$$F(x, u, y, \beta) \leq H \leq \infty,$$

integrate both sides of (3.1) and take the expectation to obtain

$$\begin{aligned} 0 &\leq \frac{EV(x(t), u(t), y(t), \beta(t))}{t} = \frac{EV(x(0), u(0), y(0), \beta(0))}{t} + \frac{1}{t} \int_0^t E(LV(x(s), u(s), y(s), \beta(s)))ds \\ &\leq \frac{EV(x(0), u(0), y(0), \beta(0))}{t} + \frac{1}{t} \int_0^t E(F(x(s), u(s), y(s), \beta(s)))ds \\ &+ 3M\sqrt[3]{\delta c_1 c_2 \lambda \sigma} E \left[\int_{-\infty}^{\infty} (x \vee 0)^{\frac{1}{3}} \pi(x) dx - \frac{1}{t} \int_0^t (\beta(s) \vee 0)^{\frac{1}{3}} ds \right] + \frac{c_1 \sigma KM}{a} \left[\frac{1}{t} \int_0^t (P(t) \vee 0) ds - \int_0^{\infty} x \widehat{\pi}(x) dx \right], \end{aligned}$$

combining $\beta(t)$ and the ergodic property of $P(t)$, it follows that

$$\lim_{t \rightarrow \infty} E \left[\int_{-\infty}^{\infty} (x \vee 0)^{\frac{1}{3}} \pi(x) dx - \frac{1}{t} \int_0^t (\beta(s) \vee 0)^{\frac{1}{3}} ds \right] = E \left[\int_0^{\infty} x^{\frac{1}{3}} \pi(x) dx \right] - \int_0^{\infty} x^{\frac{1}{3}} \pi(x) dx = 0,$$

$$\lim_{t \rightarrow \infty} E \left[\frac{1}{t} \int_0^t (P(s) \vee 0) ds - \int_0^{\infty} x \widehat{\pi}(x) dx \right] = E \left[\int_0^{\infty} x \widehat{\pi}(x) dx \right] - \int_0^{\infty} x \widehat{\pi}(x) dx = 0,$$

it can be obtained by taking the lower limit:

$$\begin{aligned} 0 &\leq \liminf_{t \rightarrow \infty} \frac{EV(x(0), u(0), y(0), \beta(0))}{t} + \liminf_{t \rightarrow \infty} \int_0^t E(F(x(s), u(s), y(s), \beta(s)))ds \\ &= \liminf_{t \rightarrow \infty} \frac{1}{t} \int_0^t E(F(x(s), u(s), y(s), \beta(s)))ds \\ &= \liminf_{t \rightarrow \infty} \frac{1}{t} \int_0^t E(F(x(s), u(s), y(s), \beta(s))) 1_{(x(s), (s), y(s), \beta(s))^T \in D_\varepsilon} ds \\ &+ \liminf_{t \rightarrow \infty} \frac{1}{t} \int_0^t E(F(x(s), u(s), y(s), \beta(s))) 1_{(x(s), (s), y(s), \beta(s))^T \in \Gamma \setminus D_\varepsilon} ds \end{aligned}$$

$$\begin{aligned} &\leq H \liminf_{t \rightarrow \infty} \frac{1}{t} \int_0^t P\{(x(s), u(s), y(s), \beta(s)) \in D_\varepsilon\} ds - \liminf_{t \rightarrow \infty} \frac{1}{t} \int_0^t P\{(x(s), u(s), y(s), \beta(s))^T \in \Gamma \setminus D_\varepsilon\} ds \\ &\leq -1 + (H + 1) \liminf_{t \rightarrow \infty} \frac{1}{t} \int_0^t P\{(x(s), u(s), y(s), \beta(s))^T \in D_\varepsilon\} ds, \end{aligned}$$

consequently

$$\liminf_{t \rightarrow \infty} \frac{1}{t} \int_0^t P(s, x(s), u(s), y(s), \beta(s), D_\varepsilon) ds \geq \frac{1}{H + 1} > 0,$$

therefore, there is a stationary distribution for the system (1.2).

4. Probability density function

The study of stationary distributions has significant implications for disease. The calculation of the density function in the vicinity of the quasi-equilibrium point in the presence of such distributions can assist in the study of the distribution of disease at a given moment in time.

First we set the quasi-equilibrium point to $(x^*, u^*, y^*, \bar{\beta})$, let $X_1 = x - x^*$, $X_2 = u - u^*$, $X_3 = y - y^*$, $X_4 = \beta - \bar{\beta}$, solving for the Jacobi matrix yields

$$\begin{pmatrix} -\beta^+ y - d & 0 & -\beta^+ x & -xy \\ \delta\beta^+ y - \frac{\eta r y}{K} & -\frac{\eta r y}{K} - (\mu + \sigma) & \delta\beta^+ x + \eta r(1 - \frac{x+u}{K}) & \delta xy \\ 0 & \sigma & -a & 0 \\ 0 & 0 & 0 & -\alpha \end{pmatrix}, \quad (4.1)$$

then the linearized system can be written as:

$$\begin{cases} dX_1 = (-a_{11}X_1 - a_{13}X_3 - a_{14}X_4)dt, \\ dX_2 = (-a_{21}X_1 - a_{22}X_2 + a_{23}X_3 + a_{24}X_4)dt, \\ dX_3 = (a_{32}X_2 - a_{33}X_3)dt, \\ dX_4 = -a_{44}X_4dt + \theta dB(t), \end{cases} \quad (4.2)$$

where

$$\begin{aligned} a_{11} &= d + \bar{\beta}y^*, \quad a_{13} = \bar{\beta}x^*, \quad a_{14} = x^*y^*, \quad a_{21} = \frac{\eta r y^*}{K} - \delta\bar{\beta}y^*, \\ a_{22} &= \frac{\eta r y^*}{K} + \mu + \sigma, \quad a_{23} = \bar{\beta}\delta x^* + \eta r(1 - \frac{x^* + u^*}{K}), \quad a_{24} = \delta x^*y^*, \quad a_{32} = \sigma, \quad a_{33} = a, \quad a_{44} = \alpha, \end{aligned}$$

rewriting the above system of equations into the form of a matrix equation

$$dX(t) = AX(t)dt + GdB(t),$$

where

$$X(t) = (X_1, X_2, X_3, X_4)^T, \quad A = \begin{pmatrix} -a_{11} & 0 & -a_{13} & -a_{14} \\ -a_{21} & -a_{22} & a_{23} & a_{24} \\ 0 & a_{32} & -a_{33} & 0 \\ 0 & 0 & 0 & -a_{44} \end{pmatrix}, \quad G = \text{diag}(0, 0, 0, \theta).$$

There exists a unique probability density function $\Phi(X_1, X_2, X_3, X_4)$ for the system in the vicinity of the quasi-equilibrium point, the form of which can be obtained by the following Fokker-Planck equation [31]:

$$\frac{\partial \Phi(X(t), t)}{\partial t} + \frac{\partial}{\partial X} [AX(t)\Phi(X(t), t)] - \frac{\theta^2}{2} \frac{\partial^2 \Phi(X(t), t)}{\partial X_4^2} = 0, \quad (4.3)$$

$\Phi(X_1, X_2, X_3, X_4)$ can be described by a quasi-Gaussian distribution

$$\Phi(X_1, X_2, X_3, X_4) = ce^{-\frac{1}{2}(X_1, X_2, X_3, X_4)P(X_1, X_2, X_3, X_4)^T},$$

where, c is a constant satisfying the normalization condition $\int_{\mathbb{R}^4} \Phi(X_1, X_2, X_3, X_4) dX_1 dX_2 dX_3 dX_4 = 1$, and the real symmetric matrix P satisfies $PG^2P + A^T P + PA = 0$, defining that $P^{-1} = \Sigma$, the above equation can be rewritten as

$$G^2 + A\Sigma + \Sigma A^T = 0. \quad (4.4)$$

Theorem 4.1 *If $R_0^s > 1$, and satisfies*

$$(d + \bar{y}^*)\left(\frac{\eta r y^*}{K} + \mu + \sigma + a\right) + a\left(\frac{\eta r y^*}{K} + \mu + \sigma\right) - \sigma[\bar{\beta}x^* + \eta r(1 - \frac{x^* + u^*}{K})] > 0,$$

$$a(d + \bar{\beta}y^*)\left(\frac{\eta r y^*}{K} + \mu + \sigma\right) - \sigma(d + \bar{\beta}y^* + \bar{\beta}x^*)[\bar{\beta}\delta x^* + \eta r(1 - \frac{x^* + u^*}{K})] > 0,$$

the normal probability density function $\Phi(x, u, y, \beta)$ of the solution of system (1.2) in the vicinity of the quasi-equilibrium point can be expressed as

$$\Phi(x, u, y, \beta) = (2\pi)^{-2} |\Sigma|^{-\frac{1}{2}} \exp\left[-\frac{1}{2}(x - x^*, u - u^*, y - y^*, \beta - \bar{\beta})\Sigma^{-1}(x - x^*, u - u^*, y - y^*, \beta - \bar{\beta})^T\right]$$

where Σ is a positive definite matrix, and

$$\Sigma = \rho_1^2(Q_1 J)^{-1} \Sigma_2 [(Q_1 J)^{-1}]^T = \rho_2^2(Q_2 L)^{-1} \Sigma_4 [(Q_2 L)^{-1}]^T,$$

$$\rho_1 = -a_{14}a_1a_6\theta, \rho_2 = -a_{14}a_2a_3\theta, J = J_3J_2J_1, L = J_4J_2J_1,$$

$$J_1 = \begin{pmatrix} 0 & 0 & 0 & 1 \\ 1 & 0 & 0 & 0 \\ 0 & 1 & 0 & 0 \\ 0 & 0 & 1 & 0 \end{pmatrix}, J_2 = \begin{pmatrix} 1 & 0 & 0 & 0 \\ 0 & 1 & 0 & 0 \\ 0 & \frac{a_{24}}{a_{14}} & 1 & 0 \\ 0 & 0 & 0 & 1 \end{pmatrix}, J_3 = \begin{pmatrix} 1 & 0 & 0 & 0 \\ 0 & 1 & 0 & 0 \\ 0 & 0 & 1 & 0 \\ 0 & 0 & -\frac{a_3}{a_1} & 1 \end{pmatrix}, J_4 = \begin{pmatrix} 1 & 0 & 0 & 0 \\ 0 & 1 & 0 & 0 \\ 0 & 0 & 0 & 1 \\ 0 & 0 & 1 & 0 \end{pmatrix},$$

$$Q_1 = \begin{pmatrix} -a_{14}a_1a_6 & a_6(a_1a_5 - a_1a_{11}) + a_1a_6a_7 & a_6(a_5^2 + a_1a_4 + a_2a_6) + a_7(a_5a_6 + a_6a_7) & t_1 \\ 0 & a_1a_6 & a_5a_6 + a_6a_7 & a_7^2 + a_2a_6 \\ 0 & 0 & a_6 & a_7 \\ 0 & 0 & 0 & 1 \end{pmatrix},$$

$$Q_2 = \begin{pmatrix} k_1 & k_2 & k_3 & k_4 \\ 0 & a_2a_3 & -a_2a_{22} - a_2a_{33} & a_{22}^2 + a_2a_{32} \\ 0 & 0 & a_2 & -a_{22} \\ 0 & 0 & 0 & 1 \end{pmatrix},$$

the exact form of Σ_2, Σ_4 will be given in the proof.

Proof. First, we determine that the matrix A is a Hurwitz matrix, computing the characteristic polynomials of A as follows:

$$\begin{aligned}\varphi_A(\lambda) &= |\lambda E - A| = \begin{vmatrix} \lambda + a_{11} & 0 & a_{13} & a_{14} \\ a_{21} & \lambda + a_{22} & -a_{23} & -a_{24} \\ 0 & -a_{32} & \lambda + a_{33} & 0 \\ 0 & 0 & 0 & \lambda + a_{44} \end{vmatrix} \\ &= (\lambda + a_{44})[\lambda^3 + (a_{11} + a_{22} + a_{33})\lambda^2 + (a_{11}a_{22} + a_{11}a_{33} + a_{22}a_{33} - a_{23}a_{32})\lambda \\ &\quad + (a_{11}a_{22}a_{33} - a_{13}a_{21}a_{32} - a_{11}a_{23}a_{32})] \\ &= (\lambda + a_{44})(\lambda^3 + d_1\lambda^2 + d_2\lambda + d_3),\end{aligned}$$

combining the conditions gives

$$d_1 > 0, d_2 > 0, d_3 > 0, d_1d_2 - d_3 > 0.$$

Take the primitive matrix $J_1 = \begin{pmatrix} 0 & 0 & 0 & 1 \\ 1 & 0 & 0 & 0 \\ 0 & 1 & 0 & 0 \\ 0 & 0 & 1 & 0 \end{pmatrix}$, calculate and obtain

$$A_1 = J_1 A J_1^{-1} = \begin{pmatrix} -a_{44} & 0 & 0 & 0 \\ -a_{14} & -a_{11} & 0 & -a_{13} \\ a_{24} & -a_{21} & -a_{22} & a_{23} \\ 0 & 0 & a_{32} & -a_{33} \end{pmatrix},$$

continuing with the elementary transformations, take the matrix $J_2 = \begin{pmatrix} 1 & 0 & 0 & 0 \\ 0 & 1 & 0 & 0 \\ 0 & \frac{a_{24}}{a_{14}} & 1 & 0 \\ 0 & 0 & 0 & 1 \end{pmatrix}$, calculate

and obtain

$$A_2 = J_2 A_1 J_2^{-1} = \begin{pmatrix} -a_{44} & 0 & 0 & 0 \\ -a_{14} & -a_{11} & 0 & -a_{13} \\ 0 & a_1 & -a_{22} & a_2 \\ 0 & a_3 & a_{32} & -a_{33} \end{pmatrix},$$

where

$$a_1 = \frac{a_{22}a_{24}}{a_{14}} - \frac{a_{11}a_{24}}{a_{14}} - a_{21}, \quad a_2 = a_{23} - \frac{a_{13}a_{24}}{a_{14}}, \quad a_3 = -\frac{a_{24}a_{32}}{a_{14}},$$

since a_3 must not be zero, we discuss whether a_1 is zero in the following:

(I) $a_1 \neq 0$

Take the primitive transformation matrix $J_3 = \begin{pmatrix} 1 & 0 & 0 & 0 \\ 0 & 1 & 0 & 0 \\ 0 & 0 & 1 & 0 \\ 0 & 0 & -\frac{a_3}{a_1} & 1 \end{pmatrix}$, calculate and obtain

$$A_3 = J_3 A_2 J_3^{-1} = \begin{pmatrix} -a_{44} & 0 & 0 & 0 \\ -a_{14} & -a_{11} & a_4 & -a_{13} \\ 0 & a_1 & a_5 & a_2 \\ 0 & 0 & a_6 & a_7 \end{pmatrix},$$

where

$$a_4 = -\frac{a_3 a_{13}}{a_1}, \quad a_5 = \frac{a_{13}(a_{23} - \frac{a_{13} - a_{24}}{a_{14}})}{a_1} - a_{22},$$

$$a_6 = a_{32} - \frac{a_3(a_{33} + a_3(\frac{a_{13} a_{24}}{a_{14}}))}{a_1} + \frac{a_3 a_{22}}{a_1}, \quad a_7 = -a_{33} - \frac{a_3(a_{23} - \frac{a_{13} a_{24}}{a_{14}})}{a_1}.$$

Noting that $J = J_3 J_2 J_1$, then Eq (4.4) can be rewritten as

$$JG^2 J^T + (JAJ^{-1})(J\Sigma J^T) + (J\Sigma J^T)(JAJ^{-1})^T = 0, \quad (4.5)$$

rewriting Eq (4.5) yields

$$G_1^2 + A_3 \Sigma_1 + \Sigma_1 A_3^T = 0,$$

let $Y_4 = X_4$, $Y_3 = a_6 X_3 + a_7 X_4$, $Y_2 = dY_3$, $Y_1 = dY_2$, so the calculation yields the standard R_1 matrix for A_3 as

$$Q_1 = \begin{pmatrix} -a_{14} a_1 a_6 & a_6(a_1 a_5 - a_1 a_{11}) + a_1 a_6 a_7 & a_6(a_5^2 + a_1 a_4 + a_2 a_6) + a_7(a_5 a_6 + a_6 a_7) & t_1 \\ 0 & a_1 a_6 & a_5 a_6 + a_6 a_7 & a_7^2 + a_2 a_6 \\ 0 & 0 & a_6 & a_7 \\ 0 & 0 & 0 & 1 \end{pmatrix}, \quad (4.6)$$

where

$$t_1 = a_7(a_7^2 + a_2 a_6) + a_6(a_2 a_5 + a_2 a_7 - a_1 a_{13}),$$

therefore, the calculation can be obtained

$$Q_1 A_3 Q_1^{-1} = \begin{pmatrix} -n_1 & -n_2 & -n_3 & -n_4 \\ 1 & 0 & 0 & 0 \\ 0 & 1 & 0 & 0 \\ 0 & 0 & 1 & 0 \end{pmatrix},$$

according to the invariance of the matrix elementary transformation, the characteristic polynomial is also invariant. Hence, we obtain

$$n_1 = a_{11} + a_{22} + a_{33} + a_{44} = d_1 + a_{44},$$

$$n_2 = a_{11} a_{33} + a_{22} a_{33} + a_{11} a_{22} - a_{23} a_{32} + a_{11} a_{44} + a_{22} a_{44} + a_{33} a_{44} = d_2 + d_1 a_{44},$$

$$n_3 = a_{11} a_{22} a_{33} - a_{13} a_{21} a_{32} - a_{11} a_{23} a_{32} + a_{11} a_{22} a_{44} + a_{11} a_{33} a_{44} + a_{22} a_{33} a_{44} - a_{23} a_{32} a_{44} = d_3 + d_2 a_{44},$$

$$n_4 = a_{11}a_{22}a_{33}a_{44} - a_{13}a_{21}a_{32}a_{44} - a_{11}a_{23}a_{32}a_{44} = d_3a_{44},$$

we can know that

$$Q_1G_1^2Q_1^T = \text{diag}((a_{14}a_1a_6\theta)^2, 0, 0, 0),$$

let

$$Q_1A_3Q_1^{-1} = D, \rho_1 = -a_{14}a_1a_6\theta, \Sigma_2 = \rho_1^{-2}Q_1\Sigma_1Q_1^T, G_0 = \text{diag}(1, 0, 0, 0),$$

rewrite the equation $Q_1G_1^2Q_1^T + (Q_1A_3Q_1^{-1})(Q_1\Sigma_1Q_1^T) + (Q_1\Sigma_1Q_1^T)(Q_1A_3Q_1^{-1})^T = 0$ to read

$$G_0^2 + D\Sigma_2 + \Sigma_2D^T = 0,$$

calculation can be obtained

$$\Sigma_2 = \begin{pmatrix} \frac{n_2n_3 - n_1n_4}{2(n_1n_2n_3 - n_3^2 - n_1^2n_4)} & 0 & -\frac{n_3}{2(n_1n_2n_3 - n_3^2 - n_1^2n_4)} & 0 \\ 0 & \frac{n_3}{2(n_1n_2n_3 - n_3^2 - n_1^2n_4)} & 0 & -\frac{n_1}{2(n_1n_2n_3 - n_3^2 - n_1^2n_4)} \\ -\frac{n_3}{2(n_1n_2n_3 - n_3^2 - n_1^2n_4)} & 0 & \frac{n_1}{2(n_1n_2n_3 - n_3^2 - n_1^2n_4)} & 0 \\ 0 & -\frac{n_1}{2(n_1n_2n_3 - n_3^2 - n_1^2n_4)} & 0 & \frac{n_1n_2 - n_3}{2n_4(n_1n_2n_3 - n_3^2 - n_1^2n_4)} \end{pmatrix}$$

computing

$$\begin{aligned} n_1n_2n_3 - n_3^2 - n_1^2n_4 &= n_1(n_2n_3 - n_1n_4) - a_3^2 \\ &= (d_1 + a_{44})(d_1d_2 - d_3)a_{44}^2 + d_3(d_1d_2 - d_3) + d_2(d_1d_2 - d_3)a_{44} > 0, \end{aligned}$$

thus, Σ_2 is a positive definite matrix, since

$$\Sigma_1 = \rho_1^2Q_1^{-1}\Sigma_2(Q_1^{-1})^T, \Sigma_1 = J\Sigma J^T,$$

therefore

$$\Sigma = \rho_1^2(Q_1J)^{-1}\Sigma_2[(Q_1J)^{-1}]^T$$

is also positive definite.

(II) $a_1 = 0$

Take the primitive transformation matrix $J_4 = \begin{pmatrix} 1 & 0 & 0 & 0 \\ 0 & 1 & 0 & 0 \\ 0 & 0 & 0 & 1 \\ 0 & 0 & 1 & 0 \end{pmatrix}$, calculate and obtain

$$A_4 = J_4A_2J_4^{-1} = \begin{pmatrix} -a_{44} & 0 & 0 & 0 \\ -a_{14} & -a_{11} & -a_{13} & 0 \\ 0 & a_3 & -a_{33} & a_{32} \\ 0 & 0 & a_2 & -a_{22} \end{pmatrix},$$

noting that $L = J_4J_2J_1$, Eq (4.4) can be rewritten as

$$LG^2L^T + (LAL^{-1})(L\Sigma L^T) + (L\Sigma L^T)(LAL^{-1})^T = 0, \quad (4.7)$$

rewriting Eq (4.7) yields

$$G_2^2 + A_4 \Sigma_3 + \Sigma_3 A_4^T = 0,$$

let $Y_4 = X_4$, $Y_3 = a_2 X_3 - a_{22} X_4$, $Y_2 = d Y_3$, $Y_1 = d Y_2$, so the calculation yields the standard R_1 matrix for A_4 as

$$Q_2 = \begin{pmatrix} k_1 & k_2 & k_3 & k_4 \\ 0 & a_2 a_3 & -a_2 a_{22} - a_2 a_{33} & a_{22}^2 + a_2 a_{32} \\ 0 & 0 & a_2 & -a_{22} \\ 0 & 0 & 0 & 1 \end{pmatrix}, \quad (4.8)$$

where

$$k_1 = -a_{14} a_2 a_3, \quad k_2 = -a_2 (a_3 a_{11} + a_3 a_{33}) - a_2 a_3 a_{22},$$

$$k_3 = a_2 (a_{33}^2 - a_3 a_{13} + a_2 a_{32}) + a_{22} (a_2 a_{22} + a_2 a_{33}), \quad k_4 = -a_{22} (a_{22}^2 + a_2 a_{32}) - a_2 (a_{22} a_{32} + a_{32} a_{33}).$$

Since, in this case, $a_1 = 0$, i.e., $a_{21} = \frac{a_{22} a_{24}}{a_{14}} - \frac{a_{11} a_{24}}{a_{14}}$, the calculation therefore reduces to

$$Q_2 A_4 Q_2^{-1} = \begin{pmatrix} -n_1 & -n_2 & -n_3 & -n_4 \\ 1 & 0 & 0 & 0 \\ 0 & 1 & 0 & 0 \\ 0 & 0 & 1 & 0 \end{pmatrix},$$

$n_1 - n_4$ is defined as above; calculate and obtain

$$Q_2 G_2^2 Q_2^T = \text{diag}((a_{14} a_2 a_3 \theta)^2, 0, 0, 0),$$

let

$$Q_2 A_4 Q_2^{-1} = D, \quad \rho_2 = -a_{14} a_2 a_3 \theta, \quad \Sigma_4 = \rho_2^{-2} Q_2 \Sigma_3 Q_2^T, \quad G_0 = \text{diag}(1, 0, 0, 0),$$

rewrite the equation $Q_2 G_2^2 Q_2^T + (Q_2 A_4 Q_2^{-1})(Q_2 \Sigma Q_2^T) + (Q_2 \Sigma Q_2^T)(Q_2 A_4 Q_2^{-1})^T = 0$ as

$$G_0^2 + D \Sigma_4 + \Sigma_4 D^T = 0,$$

the calculation gives $\Sigma_4 = \Sigma_2$; similarly, in this case

$$\Sigma_3 = \rho_2^2 Q_2^{-1} \Sigma_4 (Q_2^{-1})^T, \quad \Sigma_3 = L \Sigma L^T,$$

thus

$$\Sigma = \rho_2^2 (Q_2 L)^{-1} \Sigma_4 [(Q_2 L)^{-1}]^T$$

is also positive definite.

Combining the above two cases, the expression for the probability density function near the quasi-equilibrium point is

$$\Phi(x, u, y, \beta) = (2\pi)^{-2} |\Sigma|^{-\frac{1}{2}} \exp[-\frac{1}{2} (x - x^*, u - u^*, y - y^*, \beta - \bar{\beta}) \Sigma^{-1} (x - x^*, u - u^*, y - y^*, \beta - \bar{\beta})^T].$$

5. Disease extinction

In addition to the aforementioned considerations, the study of the conditions that lead to the extinction of infectious diseases will also play a significant role in the subsequent treatment and control of these diseases. This section will present the conditions that result in the extinction of diseases.

Theorem 5.1 *Let $(x(t), u(t), y(t), \beta(t))$ be a solution of model (1.2) with any initial value $(x(0), u(0), y(0), \beta(0))$, if*

$$R_0^e = \frac{\sigma}{\mu + \sigma} (\delta\bar{\beta}K + \eta r + \frac{\delta K \theta}{\sqrt{\pi\alpha}}) < 1,$$

then we have $\lim_{t \rightarrow \infty} u(t) = \lim_{t \rightarrow \infty} y(t) = 0$, i.e., the infection of system (1.2) will become exponentially extinct in the long run.

Proof. Constructor $W(t) = u(t) + \frac{\mu + \sigma}{\sigma} y(t)$, next we apply the Itô formula to $\ln W$,

$$\begin{aligned} L(\ln W) &= \frac{1}{W} dW = \frac{1}{W} (du + \frac{\mu + \sigma}{\sigma} dy) \\ &= \frac{1}{W} [\delta\beta^+ xy + \eta ry (1 - \frac{x+u}{K}) - (\mu + \sigma)u + (\mu + \sigma)u - \frac{(\mu + \sigma)a}{\sigma} y] \\ &\leq \frac{y}{W} [\delta\beta^+ x + \eta r - \frac{(\mu + \sigma)a}{\sigma}] \leq \frac{y}{W} [\delta\bar{\beta}x + \eta r - \frac{(\mu + \sigma)a}{\sigma}] + \frac{\delta xy}{W} (\beta^+ - \bar{\beta}) \\ &\leq \frac{\sigma}{\mu + \sigma} [\delta\bar{\beta}K + \eta r - \frac{(\mu + \sigma)a}{\sigma}] + \frac{\sigma\delta K |\beta - \bar{\beta}|}{\mu + \sigma}, \end{aligned} \quad (5.1)$$

integrating Eq (5.1) from 0 to t and dividing both sides by t yields

$$\frac{\ln W(t) - \ln W(0)}{t} \leq \frac{\sigma}{\mu + \sigma} [\delta\bar{\beta}K + \eta r - \frac{(\mu + \sigma)a}{\sigma}] + \frac{\sigma\delta K}{\mu + \sigma} (\frac{1}{t} \int_0^t |\beta(\tau) - \bar{\beta}| d\tau), \quad (5.2)$$

combining this with the powerful number theorem for martingale yields

$$\lim_{t \rightarrow \infty} \mathbb{E} (\frac{1}{t} \int_0^t |\beta(\tau) - \bar{\beta}| d\tau - \frac{\theta}{\sqrt{\pi\alpha}}) = 0, \quad (5.3)$$

taking the upper limit of Eq (5.2) and combining it with Eq (5.3) yields

$$\limsup_{t \rightarrow \infty} \frac{\ln W(t)}{t} \leq \frac{\sigma}{\mu + \sigma} [\delta\bar{\beta}K + \eta r - \frac{(\mu + \sigma)a}{\sigma}] + \frac{\sigma\delta K \theta}{(\mu + \sigma) \sqrt{\pi\alpha}} = a(R_0^e - 1) < 0, \quad (5.4)$$

where

$$R_0^e = \frac{\sigma}{\mu + \sigma} (\delta\bar{\beta}K + \eta r + \frac{\delta K \theta}{\sqrt{\pi\alpha}}) < 1.$$

Therefore, we have $\lim_{t \rightarrow \infty} W(t) = 0$, i.e., $\lim_{t \rightarrow \infty} u(t) = \lim_{t \rightarrow \infty} y(t) = 0$, implying that both latently infected as well as actively infected cells of the system (1.2) will be exponentially extinct in the long term. The theorem is proved.

6. Numerical simulation

In the numerical simulation, discretization of stochastic models is a very important and significant step, and the choice of discretization method has a great impact on the accuracy, stability, and computational efficiency of the numerical solution. The common numerical discretization methods are the Euler-Markov method and the Milstein method.

The Euler-Markov method is the simplest and most widely used method for discretizing the SDE. It is a first-order approximation that uses the discretized form of the SDE to update the solution at each step, and includes both deterministic drift and random noise terms, but its accuracy is limited to first-order convergence of the step sizes. Milstein's method is a higher-order method (second-order convergence) with a higher accuracy compared to Euler-Markov's method, and in addition to the drift and diffusion terms, Milstein's method also includes an additional term. In addition to the drift and diffusion terms, the Milstein method includes an additional term to account for the interaction between the random noise and the diffusion coefficients. This additional term improves the approximation of the solution, especially for complex SDEs where the influence of the noise term is large. In this section, we use the Milstein method [32, 33], and the discretized equations are as follows:

$$\begin{cases} x^{j+1} = x^j + \left[\lambda - dx^j - \beta^{+j}, 0x^j y^j \right] \Delta t, \\ u^{j+1} = u^j + \left[\beta^{+j} x^j y^j + \eta r y^j \left(1 - \frac{x^j + u^j}{K} \right) - (\mu + \sigma) u^j \right] \Delta t, \\ y^{j+1} = y^j + (\sigma u^j - a y^j) \Delta t, \\ \beta^{j+1} = \beta^j + \alpha [\bar{\beta} - \beta^j(t)] \Delta t + \theta \sqrt{\Delta t} \xi_j + \frac{\theta^2}{2} (\xi_j^2 - 1) \Delta t, \end{cases} \quad (6.1)$$

where, $(x^j, u^j, y^j, \beta^j)^T$ is the corresponding value for the j th iteration of Eq (6.1), Δt denotes the time increment, and ξ_j represents an independent Gaussian random variable.

Example 6.1 Select the parameter values in Table 2; in the absence of infection, the normal $CD4^+$ helper T-cell count averages 1000 *cells/mm*³ [8], and we consider a target cell carrying capacity of 800 *cells/mm*³. Calculate the conditions for the existence of a stationary distribution.

$$\hat{\beta} = \left(\frac{1}{\sqrt{\pi}} \int_{-4.4721}^{\infty} (0.002236x + 0.01)^{\frac{1}{3}} e^{-x^2} dx \right)^3 \approx 0.009914,$$

$$R_0^s = \frac{\delta \lambda \sigma \hat{\beta}}{a(\mu + \sigma) \left(d + \frac{\theta \sigma K}{2a \sqrt{\pi \alpha}} \right)} \approx \frac{0.25 \times 10 \times 0.03 \times 0.009914}{0.2 \times 0.04 \times 0.07596} \approx 1.22795 > 1,$$

calculations show that, under this set of parameters, there is a stationary distribution for system (1.2), implying that uninfected cells, latently infected cells, and actively infected cells will persist near the quasi-equilibrium point. It is clear from Figure 2 that there is a stationary distribution of the system around the quasi-equilibrium point $x^* = 63.586$, $u^* = 98.179$, $y^* = 14.727$.

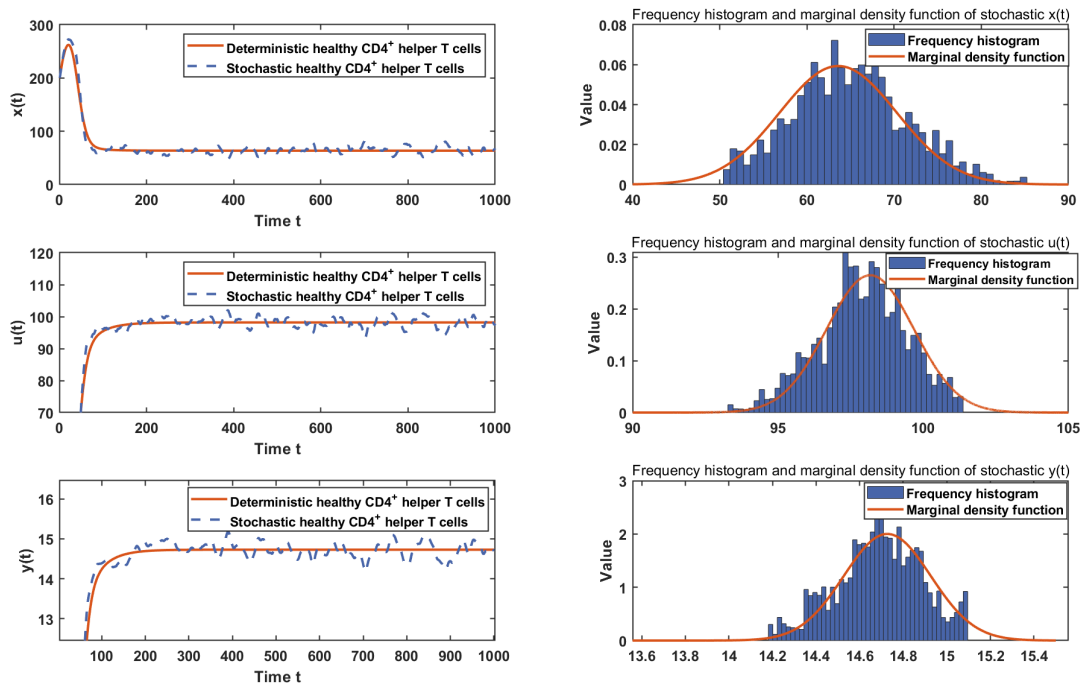


Figure 2. Stationary distribution of the system (1.2) with initial values $x(0) = 200, u(0) = 10, y(0) = 1, \beta(0) = 0.01$, left panel represents the deterministic system as well as the phenomenon of stochastic system variations, right panel represents the histogram of the frequency distribution of the stochastic system in the vicinity of the quasi-equilibrium point.

Example 6.2 In this section, we use numerical simulation to study the effect of other parameters on the system (1.2). First, we set $K = 500$, and the rest of the parameters are the same as in Table 2. Based on this, we study the effect of three different δ on the latent infected and active infected cells, $\delta = 0.04, \delta = 0.25$ and $\delta = 0.35$. Respectively, bringing them into R_0^e , we can obtain the following results:

$$\begin{aligned} \text{when } \delta = 0.04, R_0^e &= \frac{0.03}{0.04} \left(0.04 \times 0.01 \times 500 + 0.135 + \frac{0.04 \times 500 \times 0.001}{\sqrt{0.2 \times \pi}} \right) = 0.27 < 1, \\ \text{when } \delta = 0.25, R_0^e &= \frac{0.03}{0.04} \left(0.25 \times 0.01 \times 500 + 0.135 + \frac{0.25 \times 500 \times 0.001}{\sqrt{0.2 \times \pi}} \right) = 1.157 > 1, \\ \text{when } \delta = 0.35, R_0^e &= \frac{0.03}{0.04} \left(0.35 \times 0.01 \times 500 + 0.135 + \frac{0.35 \times 500 \times 0.001}{\sqrt{0.2 \times \pi}} \right) = 1.579 > 1. \end{aligned}$$

By calculating that under the first set of parameter values, the disease will go to extinction, and under the next two sets of parameter values, the disease will persist. Figure 3 illustrates this point; at the same time, looking at Figure 3, it is not difficult to see that, under the premise of the disease's persistence, with the δ getting bigger, $u(t)$ and $y(t)$ will be maintained around a larger value. Biologically speaking, the more susceptible cells become latent through infection, the more cells will be transformed into active infection, so our simulation results are reasonable.

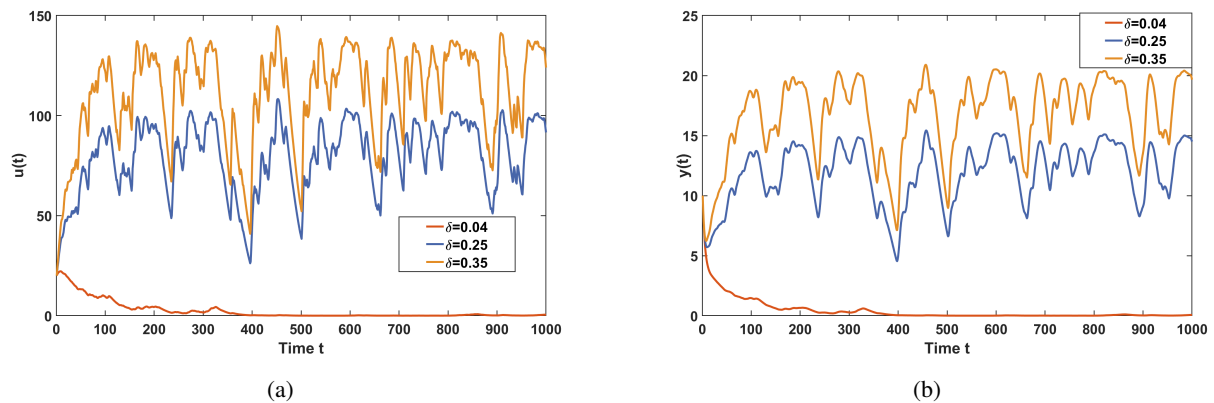


Figure 3. The state of the system (1.2) with initial values $x(0) = 50, u(0) = 20, y(0) = 10, \beta(0) = 0.01$ under different δ for $u(t)$ and $y(t)$.

Example 6.3 It is of paramount importance to study the transition time of an infected cell from its initial state $x(0), u(0), y(0)$ to a sustained state $x(s), u(s), y(s)$ and finally to an extinct state $(x(e), u(e), y(e))$, which can be referred to as the first passage time (FPT) [34]. The first passage time represents the time required for a random trajectory to reach another state for the first time; the average value of the FPT becomes the MFPT [35, 36].

In this section, we choose $N = 500$ and perform 500 cycles to obtain the average time required for the system (1.2) to reach a stationary distribution for the first time under different α and θ , respectively, with the rest of the parameters remaining the same as those in Table 2, and the plotted images are shown in Figure 4. The average time required to reach extinction for the first time in the system (1.2) with different α and θ is shown in Figure 5 for the first set of parameters chosen from Example 6.2.

Table 2. Table of parameter values.

Parameter	Value	Source	Parameter	Value	Source
λ	$10 \text{ cells}/\text{mm}^3/\text{day}$	[8, 37, 38]	$\bar{\beta}$	$0.01 \text{ cells}/\text{mm}^3/\text{day}$	[40]
d	0.01 day^{-1}	[8, 37]	δ	0.25	[8]
η	0.9	[8]	r	0.15 day^{-1}	[8]
K	$800 \text{ cells}/\text{mm}^3$	Estimated	μ	0.01 day^{-1}	[8]
σ	0.03 day^{-1}	[8]	a	0.2 day^{-1}	[36]
α	0.2 day^{-1}	[39]	θ	$10^{-3} \text{ mm}^3/\text{cells}/\text{day}^{3/2}$	[29]

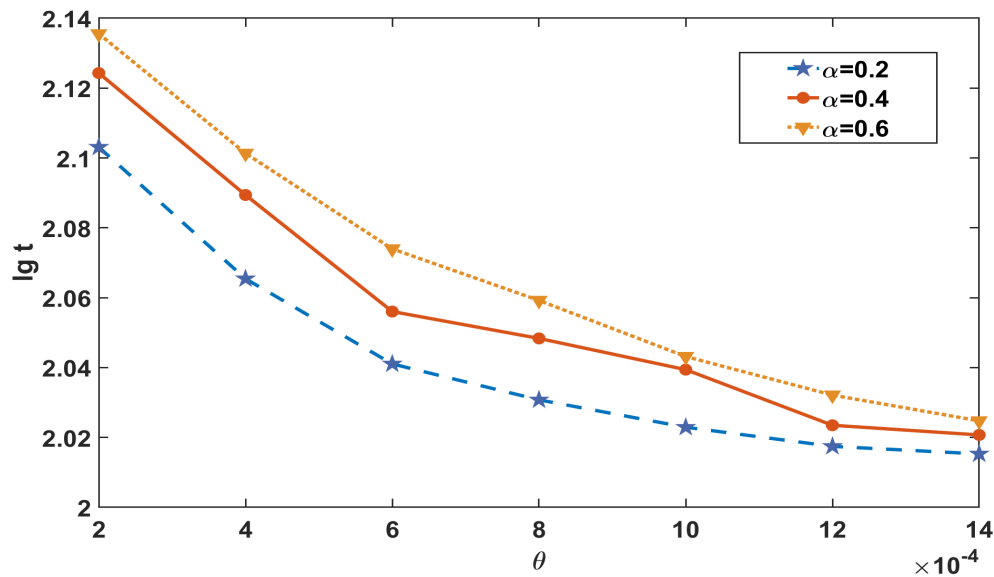


Figure 4. The average first arrival time is calculated by transferring from the initial state $(x, u, y) = (200, 10, 1)$ to the stationary distributed state $(63.586, 98.179, 14.727)$.

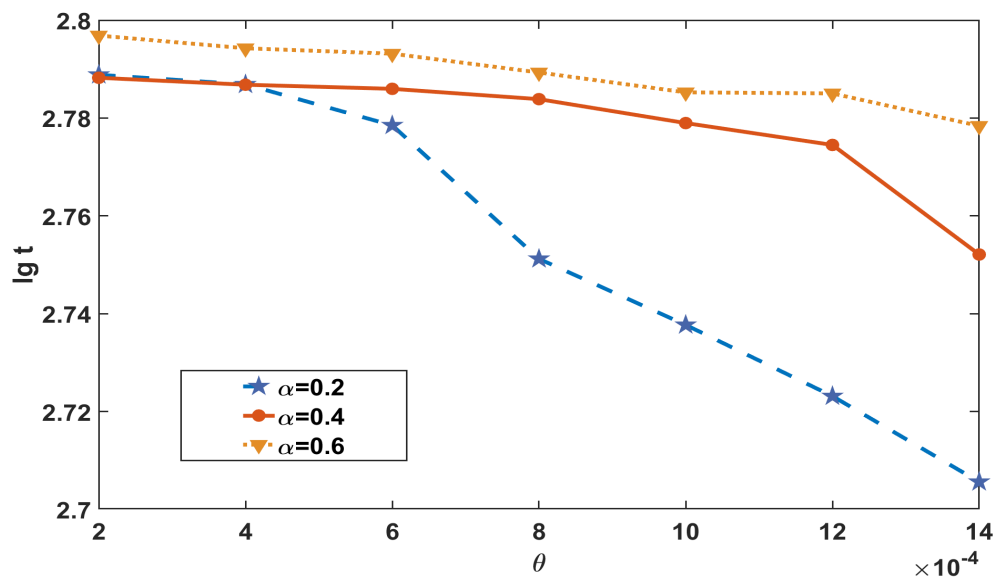


Figure 5. The average first arrival time is calculated by transferring from the initial state $(x, u, y) = (200, 10, 1)$ to the extinction state.

Example 6.4 In this section, we investigate the impact of random factors on disease extinction, maintaining all other parameters constant, and observing the change in R_0^e for different values of $[\alpha, \theta]$. As illustrated in Figure 6, R_0^e decreases as α increases or θ decreases. This implies that as the rate of regression to the mean increases or as the noise intensity decreases, the disease is effectively controlled and tends to become extinct. This is a realistic and biologically significant outcome.

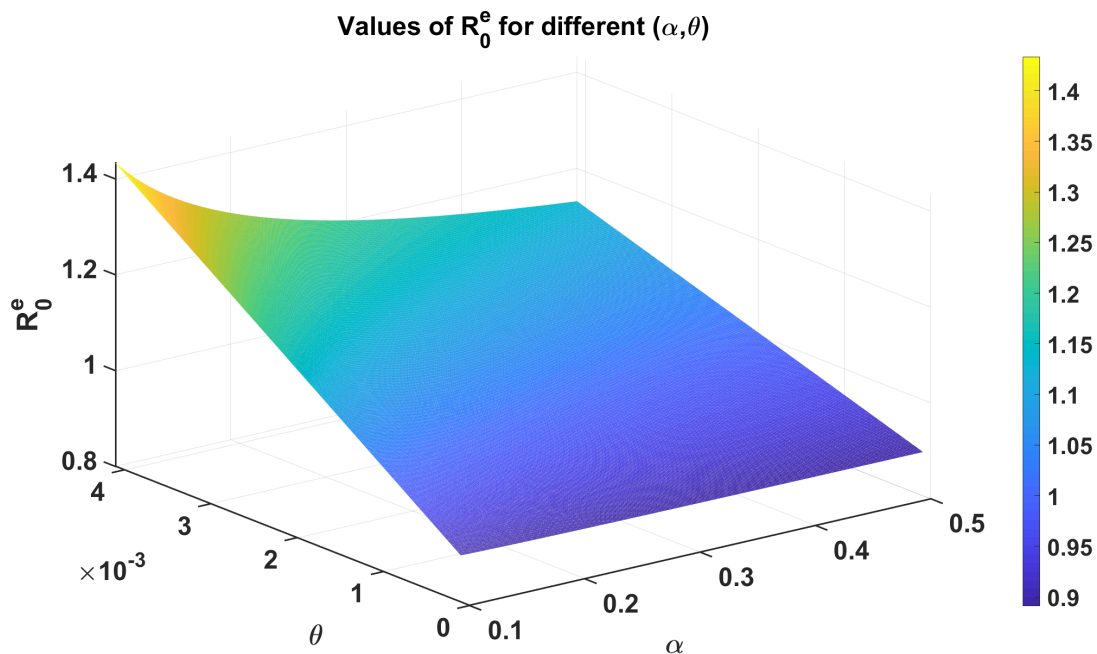


Figure 6. The color phase diagrams illustrate the variation trends of R_0^e with respect to different values of α and θ , which are constrained to the interval $[0.1, 0.5] \times [0.0001, 0.0041]$.

7. Conclusions

The objective of this paper is to investigate the dynamical impact of the Ornstein-Uhlenbeck process on the HTLV-1 model. A number of different and suitable Lyapunov functions were constructed to prove the conclusions drawn. The following paragraphs present the main results of this study:

- (i) For the stochastic model, after considering the perturbations, we show that for any initial value, there exists a unique solution to the system (1.2);
- (ii) By establishing a series of suitable Lyapunov functions, we prove the existence of a unique stationary distribution for the system at $R_0^s > 1$ and perform numerical simulations to verify the results, see Figure 2 ;
- (iii) After proving the existence of a stationary distribution, we give a concrete expression for the local normal density function corresponding to the stochastic system (1.2) in the neighborhood of the quasi-equilibrium state, provided that the conditions are satisfied;
- (iv) The threshold condition R_0^e for disease extinction is given, see Figure 3, and the effects of mean reversion rate α and noise intensity θ on this condition are also investigated, see Figure 6;
- (v) 500 simulations were performed to obtain the average elapsed time for the stochastic system to reach the stationary distribution state for the first time as well as the extinction state for different initial values as well as parameters, see Figures 4 and 5.

It is important to note that this study has certain limitations. First, we have focused on modeling the parameter infectivity β to follow the Ornstein-Uhlenbeck process. However, the model could be made more realistic by assuming that other parameters in the system (1.1) also satisfy the Ornstein-Uhlenbeck process. Moreover, we have derived local probability density expressions for the stochastic

system near the quasi-equilibrium point, but a global probability density expression remains an open question. Additionally, further investigation is needed to determine whether other types of stochastic disturbances might be more appropriate for this problem.

In the paper, we use $\beta^+ = \max\{\beta(t), 0\}$ to ensure non-negativity of the infection rate in the system. However, the non-negativity of the infection rate can also be ensured by considering the Ornstein-Uhlenbeck process that includes a logarithmic transformation, i.e., $d \ln \beta(t) = \alpha(\ln \bar{\beta} - \ln \beta(t))dt + \theta dB(t)$, for which we will carry out related work to investigate this. In addition, discussion work considering the effect of adding multiple Ornstein-Uhlenbeck processes on the model results is also underway.

Author contributions

Yan Ren: Conceptualized the study, carried out the theoretical analysis, and wrote the first draft; Yan Cheng and Yuzhen Chai: Contributed to the design of the mathematical framework and assisted with interpretation and revision; Ping Guo: Contributed to the software implementation and analysis. All authors have read and approved the final version of the manuscript for publication.

Use of AI tools declaration

The authors declare they have not used Artificial Intelligence (AI) tools in the creation of this article.

Acknowledgments

This work is supported by the Shanxi Provincial Natural Science Foundation, China (No.202303021211026); the Shanxi Province Returned Overseas Students Support Program, China (No.2023-038); the National Natural Science Foundation of China (No.12301521); Shanxi Provincial Natural Science Foundation (No.20210302124081).

Conflict of interest

The authors declare that they have no competing financial interests or personal relationships that could have appeared to influence the work reported in this paper.

References

1. E. L. Murphy, HTLV-1 and blood donation, *British J. Haemat.*, **204** (2023), 29–30. <https://doi.org/10.1111/bjh.19051>
2. N. Legrand, S. McGregor, R. Bull, S. Bajis, B. Mark Valencia, A. Ronnachit, et al. Clinical and public health implications of human t-lymphotropic virus type 1 infection, *Clinical Microb. Rev.*, **35** (2022), e0007821. <https://doi.org/10.1128/cmr.00078-21>
3. C. R. M. Bangham, HTLV-1 infections, *J. Clinic. Path.*, **53** (2000), 581–586. <https://doi.org/10.1136/jcp.53.8.581>

4. P. Katri, S. Ruan, Dynamics of human T-cell lymphotropic virus I (HTLV-I) infection of CD4+ T-cells, *Compt. Rend.-Biologies*, **327** (2004), 1009–1016. <https://doi.org/10.1016/j.crv.2004.05.011>
5. N. Ramesh, B. Cockbain, G. P. Taylor, C. Rosadas, How do socioeconomic determinants of health affect the likelihood of living with HTLV-1 globally? A systematic review with meta-analysis, *Front. Public Heal.*, **12** (2024), 1298308. <https://doi.org/10.3389/fpubh.2024.1298308>
6. G. C. L. Sampaio, J. R. Ribeiro, C. N. de Almeida, N. Boa-Sorte, B. Galvao-Castro, M. F. R. Grassi, et al. Human T cell lymphotropic virus type 1 global prevalence associated with the human development index: Systematic review with meta-analysis, *Aids Res. Human Retrov.*, **39** (2023), 145–165. <https://doi.org/10.1089/aid.2021.0230>
7. V. Soriano, C. de Mendoza, S. H. Network, Screening for HTLV-1 infection should be expanded in Europe, *Internat. J. Infect. Disease*, **140** (2024), 99–101. <https://doi.org/10.1016/j.ijid.2024.01.015>
8. M. Y. Li, A. G. Lim, Modelling the role of tax expression in HTLV-I persistence in vivo, *Bull. Math. Bio.*, **73** (2011), 3008–3029. <https://doi.org/10.1007/s11538-011-9657-1>
9. X. Zhang, M. Liu, Dynamical analysis of a stochastic delayed SIR epidemic model with vertical transmission and vaccination, *Adv. Cont. Discr. Models*, **2022** (2022), 35. <https://doi.org/10.1186/s13662-022-03707-7>
10. S. He, Y. Peng, K. Sun, SEIR modeling of the COVID-19 and its dynamics, *Nonlinear Dyn.*, **1** (2020), 1–14. <https://doi.org/10.1007/s11071-020-05743-y>
11. K. Wang, H. Fan, Y. Zhu, Dynamics and application of a generalized SIQR epidemic model with vaccination and treatment, *Appl. Math. Modell.*, **120** (2023), 382–399. <https://doi.org/10.1016/j.apm.2023.03.036>
12. W. Wang, W. B. Ma, Global dynamics of a reaction and diffusion model for an htlv-i infection with mitotic division of actively infected cells, *J. Appl. Anal. Comput.*, **7** (2017), 899–930. <https://doi.org/10.11948/2017057>
13. S. Khajanchi, S. Bera, T. K. Roy, Mathematical analysis of the global dynamics of a HTLV-I infection model, considering the role of cytotoxic T-lymphocytes, *Math. Comput. Simul.*, **180** (2021), 354–378. <https://doi.org/10.1016/j.matcom.2020.09.009>
14. Y. Wang, J. Liu, J. M. Heffernan, Viral dynamics of an HTLV-I infection model with intracellular delay and CTL immune response delay, *J. Math. Anal. Appl.*, **459** (2018), 506–527. <https://doi.org/10.1016/j.jmaa.2017.10.027>
15. V. E. Papageorgiou, P. Koliass, A novel epidemiologically informed particle filter for assessing epidemic phenomena. Application to the monkeypox outbreak of 2022, *Inverse Prob.*, **40** (2024), 035006. <https://doi.org/10.1088/1361-6420/ad1e2f>
16. D. Calvetti, A. Hoover, J. Rose, E. Somersalo, Bayesian particle filter algorithm for learning epidemic dynamics, *Inverse Prob.*, **37** (2021), 115008. <https://doi.org/10.1088/1361-6420/ac2cdc>
17. J. Elfring, E. Torta, R. van de Molengraft, Particle filters: A Hands-On tutorial, *Sensors*, **21** (2021), 438. <https://doi.org/10.3390/s21020438>
18. J. R. Artalejo, A. Economou, M. Lopez-Herrero, The stochastic SEIR model before extinction: Computational approaches, *Appl. Math. Comput.*, **265** (2015), 1026–1043. <https://doi.org/10.1016/j.amc.2015.05.141>

19. D. Li, F. Wei, X. Mao, Stationary distribution and density function of a stochastic SVIR epidemic model, *J. Franklin Inst.*, **359** (2022), 9422–9449. <https://doi.org/10.1016/j.jfranklin.2022.09.026>
20. S. Li, S. Guo, Persistence and extinction of a stochastic sis epidemic model with regime switching and levy jumps, *Disc. Contin. Dyn. Syst. Series B*, **26** (2021), 5101–5134. <https://doi.org/10.3934/dcdsb.2020335>
21. Z. Ni, D. Jiang, Z. Cao, X. Mu, Analysis of stochastic SIRC model with cross immunity based on Ornstein-Uhlenbeck process, *Qual. Theory Dyn. Syst.*, **22** (2023). <https://doi.org/10.1007/s12346-023-00782-3>
22. Edward Allen, Environmental variability and mean-reverting processes, *Disc. Contin. Dyn. Syst. Series B*, **21** (2016), 2073–2089. <https://doi.org/10.3934/dcdsb.2016037>
23. B. Zhou, D. Jiang, B. Han, T. Hayat, Threshold dynamics and density function of a stochastic epidemic model with media coverage and mean-reverting Ornstein-Uhlenbeck process, *Math. Comput. Simulation*, **196** (2022), 15–44. <https://doi.org/10.1016/j.matcom.2022.01.014>
24. Y. Cai, J. Jiao, Z. Gui, Y. Liu, Y. Liu, Environmental variability in a stochastic epidemic model, *Appl. Math. Comput.*, **329** (2018), 210–226. <https://doi.org/10.1016/j.amc.2018.02.009>
25. T. Su, Q. Yang, X. Zhang, D. Jiang, Stationary distribution, extinction and probability density function of a stochastic SEIV epidemic model with general incidence and Ornstein-Uhlenbeck process, *Phys. A: Stat. Mech. Appl.*, **615** (2023), 128605. <https://doi.org/10.1016/j.physa.2023.128605>
26. Z. Shi, D. Jiang, Environmental variability in a stochastic HIV infection model, *Commun. Nonlinear Sci. Numer. Simul.*, **120** (2023), 107201. <https://doi.org/10.1016/j.cnsns.2023.107201>
27. Q. Liu, D. Jiang, Analysis of a stochastic logistic model with diffusion and Ornstein-Uhlenbeck process, *J. Math. Phys.*, **63** (2022), 53505. <https://doi.org/10.1063/5.0082036>
28. J. Shang, W. Li, Dynamical behaviors of a stochastic SIRV epidemic model with the Ornstein-Uhlenbeck process, *Adv. Contin. Discrete Model.*, **2024** (2024), 9. <https://doi.org/10.1186/s13662-024-03807-6>
29. Q. Liu, Dynamical analysis of a stochastic maize streak virus epidemic model with logarithmic Ornstein-Uhlenbeck process, *J. Math. Bio.*, **89** (2024), 30. <https://doi.org/10.1007/s00285-024-02127-3>
30. X. Mao, *Stochastic differential equations and applications*, Elsevier, 2007. <https://doi.org/10.1533/9780857099402>
31. C. W. Gardiner, Handbook of stochastic methods for physics, chemistry and the natural sciences, *Springer Ser. Syn.*, 1985. <https://doi.org/10.1002/phbl.19860420812>
32. B. Zhou, D. Jiang, Y. Dai, T. Hayat, Stationary distribution and density function expression for a stochastic SIQRS epidemic model with temporary immunity, *Nonlinear Dyn.*, **105** (2021), 931–955. <https://doi.org/10.1007/s11071-020-06151-y>
33. D. J. Higham, An algorithmic introduction to numerical simulation of stochastic differential equations, *SIAM Rev.*, **43** (2001), 525–546. <https://doi.org/10.1137/s0036144500378302>
34. J. Duan, *An introduction to stochastic dynamics*, Cambridge University Press, 2015.

35. A. Yang, H. Wang, T. Zhang, S. Yuan, Stochastic switches of eutrophication and oligotrophication: Modeling extreme weather via non-Gaussian Levy noise, *Chaos*, **32** (2022), 1–15. <https://doi.org/10.1063/5.0085560>
36. Z. Shi, D. Jiang, Dynamical behaviors of a stochastic HTLV-I infection model with general infection form and Ornstein-Uhlenbeck process, *Chaos Solit. Fract.*, **165** (2022), 112789. <https://doi.org/10.1016/j.chaos.2022.112789>
37. C. Song, R. Xu, Mathematical analysis of an htlv-i infection model with the mitosis of cd4+ t cells and delayed ctl immune response(Article), *Nonlinear Anal.: Modell. Control*, **26** (2021), 1–20. <https://doi.org/10.15388/namc.2021.26.21050>
38. A. M. Elaiw, N. H. AlShamrani, Analysis of a within-host HIV/HTLV-I co-infection model with immunity, *Virus Res.*, **295** (2021), 198204. <https://doi.org/10.1016/j.virusres.2020.198204>
39. Q. Liu, Stationary distribution and probability density for a stochastic SISP respiratory disease model with Ornstein-Uhlenbeck process, *Commun. Nonlinear Sci. Num. Simul.*, **119** (2023), 107128. <https://doi.org/10.1016/j.cnsns.2023.107128>
40. D. Kuang, Q. Yin, J. Li, Dynamics of stochastic HTLV-I infection model with nonlinear CTL immune response, *Math. Meth. Appl. Sci.*, **44** (2021), 14059–14078. <https://doi.org/10.1002/mma.7674>



AIMS Press

©2024 the Author(s), licensee AIMS Press. This is an open access article distributed under the terms of the Creative Commons Attribution License (<http://creativecommons.org/licenses/by/4.0>)